

# THE DEFLECTION PLATE ANALYZER: A TECHNIQUE FOR SPACE PLASMA MEASUREMENTS UNDER HIGHLY DISTURBED CONDITIONS

**Kenneth H. Wright, Jr.**

NASA/MSFC, Mail Stop: SD50  
National Space Science Technology Center  
320 Sparkman Dr., Huntsville, AL 35805  
Phone: 256-961-7648  
Fax: 256-961-7216  
E-mail: [Kenneth.H.Wright@nasa.gov](mailto:Kenneth.H.Wright@nasa.gov)

**Ken Dutton**

Madison Research Corporation

**Nelson Martinez**

**Dennis Smith**  
NASA/MSFC

**Nobie H. Stone**

SRS System Technology Group

## **Abstract**

A technique has been developed to measure the characteristics of space plasmas under highly disturbed conditions; e.g., non-Maxwellian plasmas with strong drifting populations and plasmas contaminated by spacecraft outgassing. The present method is an extension of the capabilities of the Differential Ion Flux Probe (DIFP) to include a mass measurement that does not include either high voltage or contamination sensitive devices such as channeltron electron multipliers or microchannel plates. This reduces the complexity and expense of instrument fabrication, testing, and integration of flight hardware as compared to classical mass analyzers. The new instrument design is called the Deflection Plate Analyzer (DPA) and can deconvolve multiple ion streams and analyze each stream for ion flux intensity (density), velocity (including direction of motion), mass, and temperature (or energy distribution). The basic functionality of the DPA is discussed. The performance characteristics of a flight instrument as built for an electrodynamic tether mission, the Propulsive Small Expendable Deployer System (ProSEDS), and the instrument's role in measuring key experimental conditions are also discussed.

## **Introduction**

The technique described in this paper is derived from the basic Differential Ion Flux Probe (DIFP) instrument. The DIFP is a scientific instrument capable of deconvolving several coincident ion streams, differing in flow direction and/or energy, and independently determining the flow direction, current density, and energy distribution of each stream.<sup>1</sup> The DIFP was developed for laboratory investigations in the area of plasma-body interactions<sup>2,3,4</sup> and later upgraded for flight on the STS-3 and Spacelab-2 shuttle missions and for flight aboard the CENTAUR-I and -II sounding rockets.<sup>5</sup> On the Spacelab-2 mission, the DIFP performed the

first in situ differential, vector measurements of ion streams in the disturbed, non-parallel flow produced in the wake of an ionospheric satellite.<sup>6</sup> A similar instrument was used to diagnose the highly disturbed plasma, such as ion reflection from a positive sheath, surrounding the tether satellite during the TSS-1 and TSS-1R missions.<sup>7,8,9</sup>

With our improved comprehension of the complexity of plasma processes involved in the earth's magnetosphere and the local, perturbed environment of a spacecraft, the need for sophisticated measurements and a more careful assessment of spacecraft environmental effects has become apparent. For example, it appears that spacecraft charging effects were erroneously interpreted as either a wake traversal of the satellite Ganymede or a "bubbling" state of the Jovian magnetospheric plasma.<sup>10</sup> The effect of spacecraft-space plasma interactions was further emphasized by the results of the STS-3 and Spacelab-2 missions, where outgassed contaminants produced a co-orbiting neutral gas cloud that surrounded the space shuttle and significantly modified the physics of its interaction with the ionosphere.<sup>11,12</sup> In addition, active experiments that involve perturbing influences, such as charge particle beam injection, high power rf wave injections, and electrodynamic tethers that use plasma contactors must deal with situations that represent strong departures from the ambient conditions for which the typical plasma instrumentation is designed.

In the geophysical context, strong evidence has been presented in recent years that the "core plasma" population in the terrestrial magnetosphere results from the plasma outflows that occur in the high-latitude polar ionosphere.<sup>13</sup> Spacecraft that are positioned to study these processes pass through highly disturbed, non-equilibrium plasmas and require the type of instrumentation examined herein. For example, this instrument can provide measurements of the early development of ion conics in the ionospheric plasma and is able to deconvolve these effects from those effects associated with spacecraft charging.<sup>14,15</sup>

### **Measurement Concept**

The original DIFP sensor head consisted of an electrostatic deflection and collimation system mounted in front of a planar, gridded retarding potential analyzer (RPA). As shown in Figure 1, a stream of ions arriving at the entrance slit with some angle of attack,  $\Theta$ , which lies in a plane perpendicular to the collimation slits (the "analysis plane"), and with some energy,  $E$ , will be deflected through the exit slit by applying a specific potential,  $\Phi_d$ , of opposite polarity to the deflection plates. Note that in the original design, only the components of the ion velocity vector lying in the analysis plane could be analyzed.

At any given deflection potential, the instantaneous field of view in the analysis plane is limited by the geometry of the deflection and collimation system to approximately  $\Delta\Theta$  (there is a second-order increase with  $\Phi_d$ ). Therefore, by sweeping  $\Phi_d$ , the DIFP can differentially scan over the angular range of  $\pm\Omega$ . If the ion energy is increased, a higher potential must be applied to the plates to deflect the ions the same amount for any value of  $\Theta$ . Therefore, the electrostatic deflection and collimation system can be viewed as an energy-angle filter which operates such that at any given deflection potential,  $\Phi_d$ , the energy and angle of the admissible ion must satisfy a known relation,  $f(\Theta, E) = \Phi_d$ , where the function  $f$  is a characteristic of the deflection and collimation system design.

After passing through the deflection and collimation system, the ions enter the Retarding Potential Analyzer (RPA) section at an angle  $\alpha$ , which is much smaller than  $\Theta$ . Their energy, due to the velocity component normal to the grids, is proportional to the potential at which the ions are retarded and can, therefore, be determined by sweeping the retarding potential,  $\Phi_r$ . The measured values of  $\Phi_d$  and  $\Phi_r$  then provide two known variables that can be used to determine the two unknown characteristics of the ions,  $\Theta$  and  $E$ .

### **Functional Description of the New Technique**

The new method is basically a modified and enhanced version of the previous DIFP. The measurement capabilities are expanded to include (1) all three components of the ion velocity vector and (2) ion mass analysis. Figure 2 shows a functional schematic of the new design, the Deflection Plate Analyzer (DPA).

The ion optics from the earlier design remain divided into an angle selection system and an energy (plus mass) system. However, to resolve all three velocity components, the angle selection system has been modified to include two pairs of orthogonal deflection plates beneath the entrance aperture. The lower panel in Figure 2 shows the angle selection system as viewed from the top along the instrument axis. By sweeping an applied voltage to the pair of deflection plates labeled 1, with polarity indicated, the ion stream moves along the X-direction until the ion stream hits the angle locator bar. At this point the voltage on deflection pair 1 is held constant ( $\Phi_X$ ) while the voltage applied to deflection pair 2 is swept, with the indicated polarity. The ion stream moves along the locator bar in the Y-direction until the hole is encountered, thereby deflecting the ion stream down the sensor axis. At this point, the voltage on deflection pair 2 is held constant ( $\Phi_Y$ ).

In the energy/mass analysis section, the grids from the earlier design have been replaced by a series of four deflection plates. For a unique voltage  $\Phi_{E,M}$  and polarity between the plates, as shown in the top panel of Figure 2, the ion stream will execute a “dog-leg” path. Because the ions, in this section, travel parallel to the instrument axis (i.e., there is no angular variation), the voltage required to deflect the ions,  $\Phi_{E,M}$ , is directly proportional to the ion drift energy,  $E$ ; i.e.  $\Phi_{E,M} = \beta E$ , where  $\beta$  is proportional to the deflection angle. For a typical design, the deflection angle is approximately  $15^\circ$  and  $\beta \approx 0.2 - 0.3$ . For the RPA design of the DIFP,  $\beta = 1$  since the ions had to be completely retarded at some point. In the Deflection Plate Analyzer, ions are merely deflected through a curved path, therefore, requiring less voltage, which increases the energy range for a given voltage.

If the bias voltage  $\Phi_{E,M}$  is modulated, the ion stream can be “gated” between the plates to provide a time-of-flight measurement for ion velocity and, therefore, mass. The modulation will cause the stream to execute either of the two trajectories shown in the top panel of Figure 2. Summing the two alternating paths increases the instrument's throughput. A unique frequency can be found that allows the ion stream to pass through the instrument and reach the collector. Time-of-flight (and, therefore, ionic mass) is inversely proportion to this frequency.

The operation of the DPA provides the following six known measurement values: collected ion current, angle deflection voltage  $\Phi_X$ , angle deflection voltage  $\Phi_Y$ , energy deflection voltage

$\Phi_E$ , width of energy response curve, and modulation frequency. These values can be used to solve for the six unknown properties of each ion component of the plasma: ion stream density, angles-of-incidence (azimuth  $\theta_X$  and pitch  $\theta_Y$  relative to the instrument normal) and ionic drift energy, temperature, and mass.

An early flight version of the DPA was built and tested as part of the Plasma Experiment Satellite Test that was flown as part of the Joint Air Force Weber State Satellite in January 2000. A malfunction on the satellite prevented the power up of the experiment. However, the information gained in development of a flight version of the instrument lead to design changes for an improved flight instrument described below.

### **Flight Instrument Development**

A potential opportunity for flight validation of the DPA technique arose on the Propulsive Small Expendable Deployer System (ProSEDS) mission. ProSEDS is designed to provide an on-orbit demonstration of the propulsion capabilities of electrodynamic tethers in space.<sup>16</sup> The motion of the 5-km conducting bare tether through the magnetized ionospheric plasma will transform orbital kinetic energy into electrical power resulting in the collection of multi-Amp currents. This loss of orbital energy, due to the decelerating force produced by the interaction of the tether current with the Earth's magnetic field, will lower the orbit much faster than what results from aerodynamic drag alone. ProSEDS is a secondary payload on a Delta-II expendable rocket.

The DPA provides three critical measurements of the experimental conditions during various tether circuit operational sequences. (1) It will provide a measurement of the background ionospheric plasma density. (2) It will provide a reliable measure of the potential between the Delta stage and the surrounding ionospheric plasma. This plasma sheath results from the operation of a hollow cathode plasma contactor as it returns the tether current to the ionosphere. Determination of the sheath potential is accomplished by measuring the energy of the ions accelerated into the sensor by this potential. The geometry and size of the Delta stage's plasma sheath, therefore, do not effect the measurement. (3) The emission of ionized Xenon gas by the plasma contactor will contaminate the local ionospheric plasma. The DPA, with its mass analysis capability, will measure the composition of the environmental plasma. The presence or absence of Xenon ions will be determined and used to access the quality of the ambient plasma measurements.

Note: In published ProSEDS papers and internal documentation, this instrument is denoted as the Differential Ion Flux Probe w/Mass analysis (DIFPM). Our preferred name for the instrument is the DPA, as used in this paper.

### **Ion optics**

Figure 3 illustrates the packaging of the DPA ion optics stack. The housing consists of three parts that contain the five deflection plates necessary for control of the ion trajectory through the stack. Each deflection plate is fabricated from a ceramic. A gold paste is "fired" onto the surface to provide the necessary conductive areas; i.e., ground planes, signal traces, and

electrodes. The dimension of the entrance aperture is 0.050 in by 0.050 in. The overall dimensions of the cylindrical ion optics stack are roughly 1.5 in diameter by 2.5 in long. Attached to the bottom of the stack (not shown) is a housing containing two electrometer circuits (including pre-amps) that serve the collector plate and the angle locator bar. Each electrometer is sensitive down to the pico-Amp current range and has two gain ranges. The throughput for the ion optics stack is 18%. The ion optics stack and the electrometer package constitute the DPA sensor. For comparison, the throughput value for the DIFP sensor used on the Spacelab-2 and TSS missions was 35%. The increased functionality of the DPA was achieved at a decrease by a factor of 2 in throughput.

## Operational control

A separate electronics box provides the sweep voltages and electrometer control signals to the sensor. The sensor(s) plus the electronics box comprise the instrument package. The power and data interface is also through this electronics box. The operational control of the different measurement sequences of the sensor is accomplished through the use of two micro-controller integrated circuit chips. These chips have the capability to be reprogrammed in real-time which allows for a drastically easier effort in fine-tuning the control software during vacuum plasma tests of the instrument.

The operation of the DPA is a specific application of the measurement sequence described in the previous section. Initially, a 128-point bi-polar voltage sweep in X is performed. The voltage locations ( $\Phi_X$ ) for up to 10 current peaks are stored. These are ordered with respect to decreasing current (high to low). The number ten is chosen to accommodate for noise, i.e., false positives. The current measured for the X-voltage sweep is the sum of the collector and locator bar responses. Current peak detection is performed via software. After the X-sweep and current peak ordering is completed, further analysis is performed on the three highest current peaks. For each current peak, a 128-point bi-polar voltage sweep in Y is performed. The current monitored in this case is only from the collector. The voltage location ( $\Phi_Y$ ) at the current peak is stored. The voltage pair ( $\Phi_X, \Phi_Y$ ) is applied to the entrance deflection plates and held constant while a 99-point bi-polar voltage is swept for the energy analysis (E-sweep). The voltage location ( $\Phi_E$ ) for the current peak is stored and used for the mass analysis. The  $\Phi_E$  voltage serves as the amplitude of a square wave for a 99-point frequency sweep from 100kHz to 2 MHz (M-sweep). The frequency values ( $F_M$ ) for up to four current peaks are stored. Figure 4 shows the response for each of the four operations described above.

To minimize the size of the telemetry, the voltage-current (V,I) response for each operation is not stored. The nominal telemetry frame consists of ( $\Phi_X, I$ ) for each peak in the X-sweep; ( $\Phi_Y, I$ ) for the peak in the Y-sweep; all 99 I-values for the E-sweep; and ( $F_M, I$ ) for the peaks in the M-sweep. At regular intervals, a "calibration" telemetry frame is returned. This frame consists of the information in the nominal telemetry frame plus the (V,I) values for the X-sweep, Y-sweep, and M-sweep.

The DPA instrument can operate in a single, automated analysis mode that will determine all of the plasma properties for several ion streams. The time for analysis of a single ion stream is about one second. Obviously, if a faster response is needed the number of points in the various

sweeps can be reduced. Depending on the science objective, the proper trade can be made between speed and resolution (voltage range and voltage step size).

### Calibration data

Functional testing and calibration of the DPA was performed in the Space Plasma Physics Laboratory of the Space Science Department at the National Space Science and Technology Center. The test facility is comprised of a Kaufman ion thruster attached to a 4 ft x 8 ft vacuum chamber that is evacuated with an oil-free pumping system (both roughing and high-vacuum). The system operating pressure during plasma testing was  $7-8 \times 10^{-6}$  Torr. A mounting table attached to a mechanical, rotating feed through allowed for the angular characteristics of the DPA to be determined. The ion component of the plasma stream has typical properties of 10s of eV drift energy with a temperature in the drift direction of 300 K – 500 K.

Figure 5 shows the calibration data for the angle, energy, and mass (velocity) operations. The equations used to derive the various plasma quantities are given by:

(1) Angle:  $\theta_X, \theta_Y$  (deg) =  $30\Phi + 0.48\sin^{-1}(0.8\Phi)$ , where  $\Phi \equiv \varphi_{X,Y} / E$

(2) Angular sensitivity: for  $\theta_{X,Y}$  (deg)  $\leq 17^\circ$ :  $g = \exp(-2.63 \times 10^{-3}\theta^2 + 1.0 \times 10^{-6}\theta^4)$   
for  $\theta$  (deg)  $> 17^\circ$ :  $g = 0.0441\cos^2\theta + 0.565\cos^4\theta$

(3) Energy:  $E(\text{eV}) = 4.0\varphi_E(\text{V})$

(4) Velocity:  $V(\text{km/s}) = [F(\text{kHz}) + 10.5]/51.7$ , where  $F \equiv$  frequency @ peak

(5) Mass:  $M(\text{amu}) = 193[E(\text{eV})/V^2(\text{km/s})]$

(6) Density:  $N(\#/ \text{cm}^{-3}) = 2.04 \times 10^{16} [I_0(\text{Amps}) / V(\text{km/s})]$ , where  
 $I_0(\text{Amps}) = I_Y(\text{Amps}) / [g(\theta_X) * g(\theta_Y)]$

Using the above equations and other instrument parameters, the performance characteristics for the present DPA instrument can be stated as - ambient ionospheric density:  $4.4 \times 10^3 - 3.9 \times 10^6 \text{ cm}^{-3}$ ; energy range: up to 100 eV; ion flow direction: +/- 60 deg for both X- and Y- directions; and deconvolve multiple streams at normal incidence with 3 deg resolution. For Xenon neutrals from the hollow cathode that ionize via the pick-up process, the DPA can diagnose them over the velocity range  $0.35V_{\text{orb}} - 1.55V_{\text{orb}}$  where  $V_{\text{orb}} = 7.8 \text{ km/s}$ . Recall the pick-up process produces ions with velocities ranging from 0 to  $2V_{\text{orb}}$ .

### Two-stream data

To illustrate the multiple stream diagnosis capability of the DPA, data from a test set-up where a biased cylinder was placed in front of the sensor was obtained. This is shown in Figure 6. The cylinder was biased to  $\sim -18\text{V}$ . The X-sweep clearly identifies two streams. For each of these streams the Y-, E-, and M-Sweep data is shown. Since the energy and mass of each stream are equal by definition, the curves from each of these sweeps overlay each other. Differences are

due to differing trajectory paths through the ion optics. The asymmetry of the current in the Y-sweep is due to the physical details of the aperture in the angle locator bar (see Figure 2). Also of note is that sometimes the peak value of current in the Y-sweep does not equal the peak current value of the middle peak in the E-sweep. This effect can introduce second order corrections to the density. The reasons for the difference lies in the  $\Phi_Y$  sweep and the dwell time for the voltage step versus the fixed  $\Phi_Y$  and dwell time for the  $\Phi_E$  voltage step.

### **ProSEDS system test**

The DPA participated in a system test under vacuum to verify proper functioning of the complete system to the fullest extent possible. A simulated emf could be imposed on the system resulting in current flow in the circuit. The hollow cathode was operated thereby emitting a Xenon plasma. The vacuum chamber had no background plasma so closure of the hollow cathode current was accomplished via an anode plate located near the orifice of the hollow cathode. The DPA sensors were located approximately a meter away from the plasma column and oriented such that any  $Xe^+$  ions emitted perpendicular to the column could be detected. Figure 7a shows the three sensors mounted for the test. The various operational sequences of the tether circuit were exercised which resulted in various levels of  $Xe^+$  ion flux emitted from the plasma column. Data from the middle sensor in Figure 7a of the  $Xe^+$  ions for two circuit configuration are shown in Figure 7b. In the shunt mode, a 15-ohm resistor is placed in the circuit. In the second mode, a load resistor of 2200-ohm is placed in the circuit while the emf remains constant. More of the emf is used to support the voltage drop across the load resistor resulting in less current and hence, less ionization in the plasma column between the hollow cathode and the anode plate.

### **Summary**

A new technique for measuring disturbed plasmas has been discussed. The technique is an extension of a method began by our group in the 1970's to diagnose the complex plasma behavior of the wakes of bodies in flowing plasmas. A new flight instrument has been developed and is quite rugged, judged by the fact that it has survived severe environmental testing – random vibration levels of 27.5 g rms and a temperature range of -40C to 85C. The capabilities of the instrument are well suited to active spacecraft experiments and electrodynamic tethers (such as ProSEDS) – in particular its ability to distinguish between the ambient ionospheric plasma and the spacecraft generated plasma. The DPA angle discrimination ability makes it a good candidate instrument for use both in the high latitude ionosphere and for inferring  $ExB$  drifts from ram deviated flows (in the case of high angular resolution). Future enhancements to the instrument involve (1) miniaturizing the control electronics packaging such that it can be contained in a small volume at the end of ion optics stack; and (2) improving the resolution at low energy by removing the central peak in the energy sweep response.

### **Acknowledgement**

The authors would like to acknowledge the contributions of Cynthia Ferguson and John Redmon of NASA/MSFC to the mechanical design of the flight DPA.

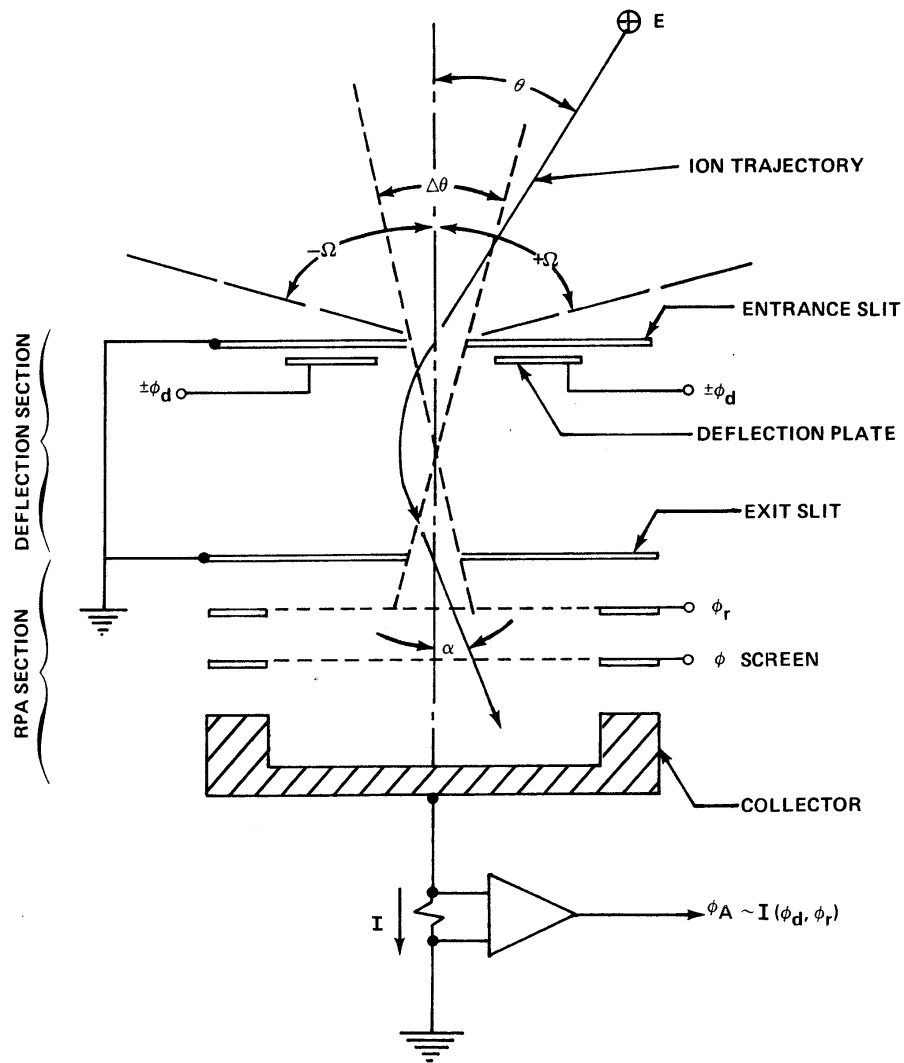


Figure 1. DIFP functional schematic showing a cut through the instrument in a plane normal to the deflection system entrance aperture.<sup>1</sup>

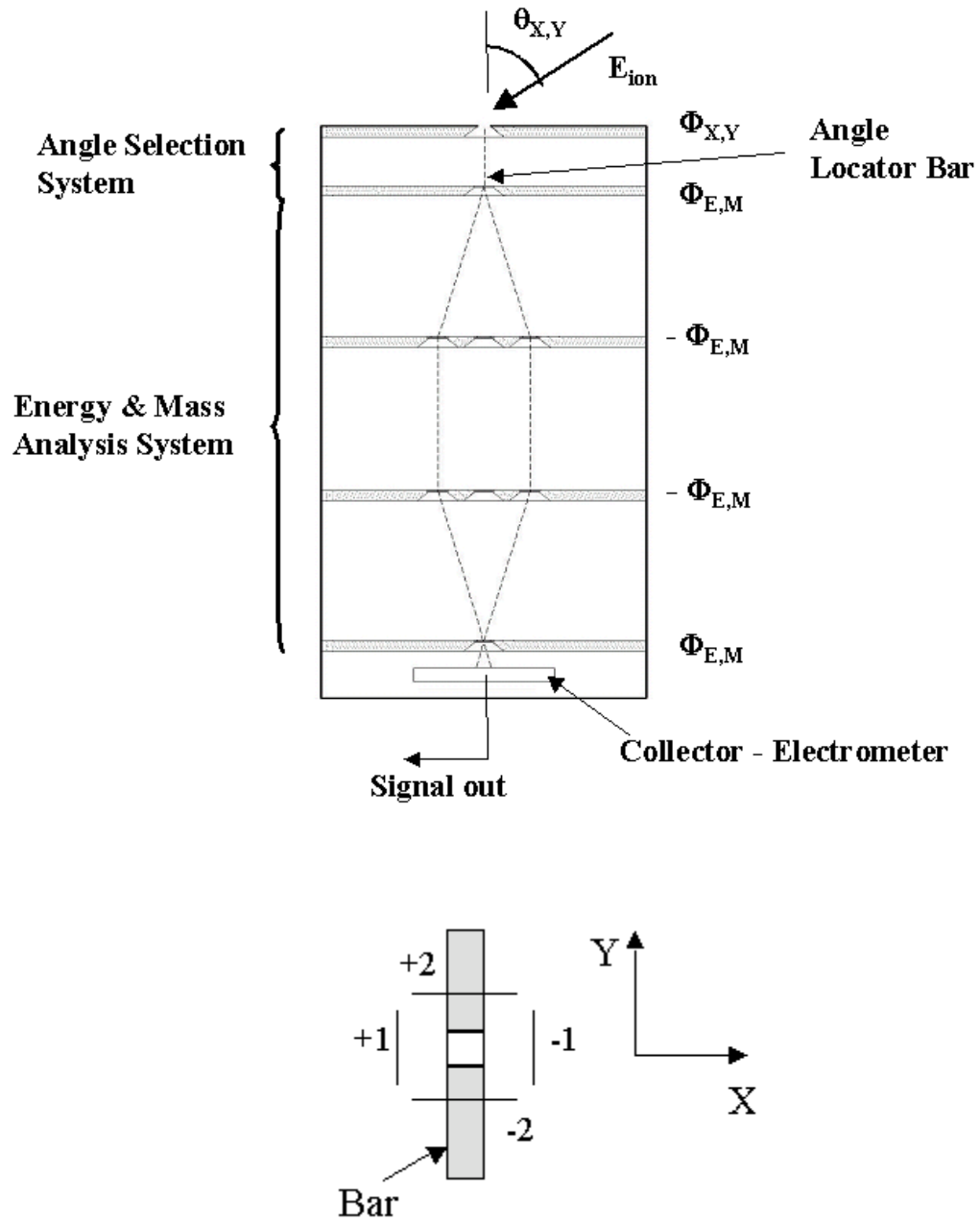
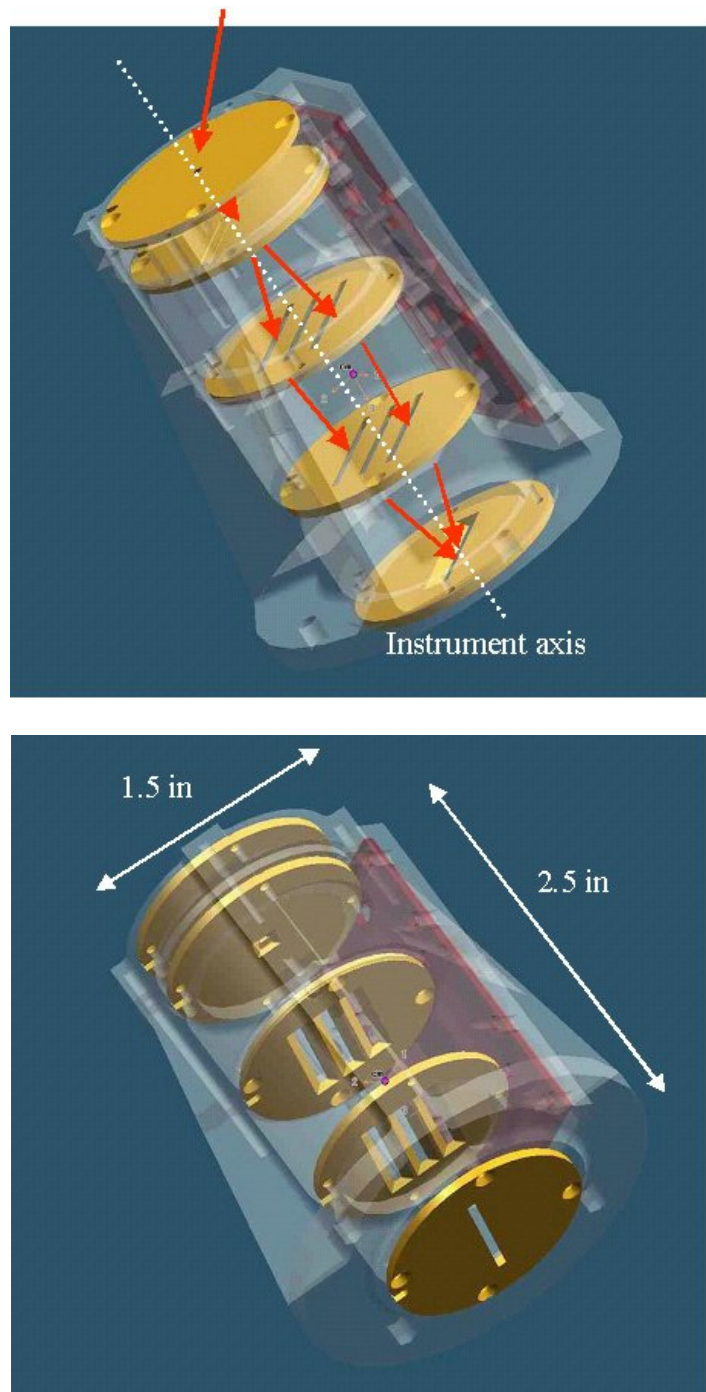
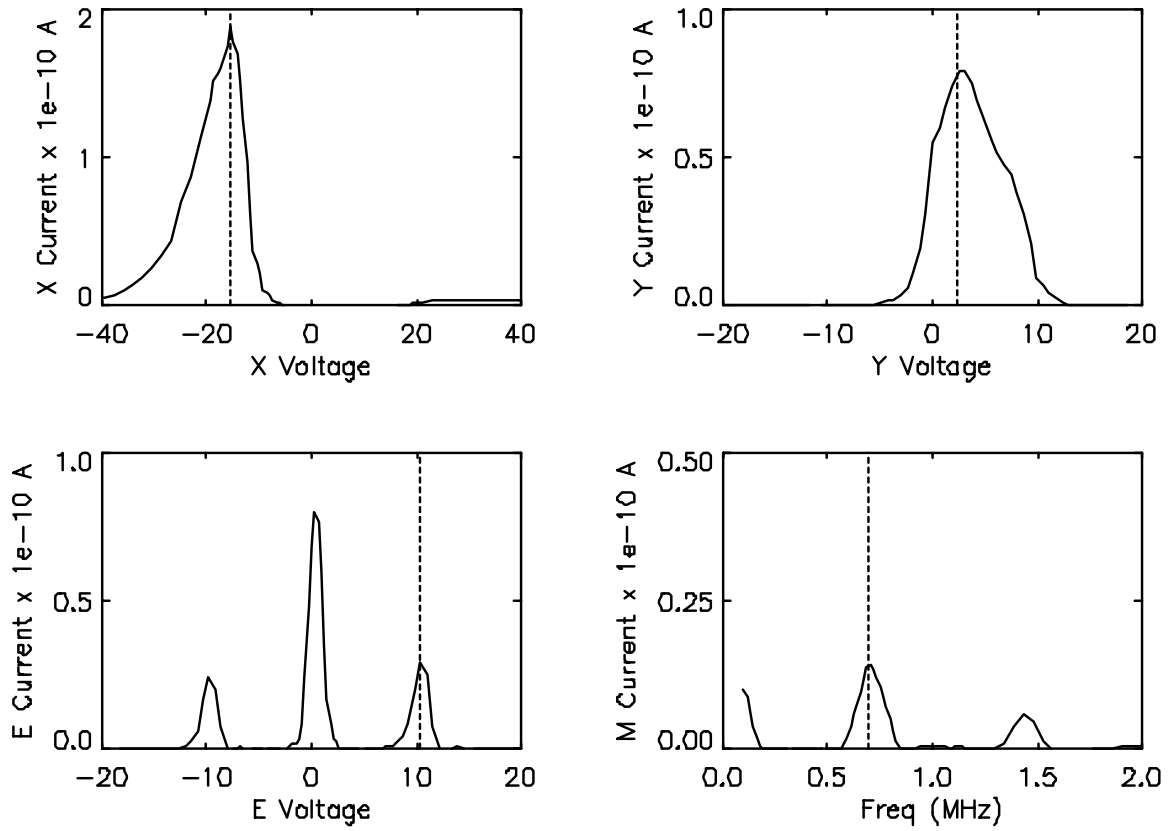


Figure 2. DPA functional schematic. The upper panel shows a cut through the instrument in a plane normal to the entrance aperture. The lower panel shows an exaggerated view of the angle locator bar and the projection of the deflection plates of the entrance aperture.



**Figure 3. DPA ion optics stack. Upper panel: ion trajectory into and through instrument. Lower panel: view illustrating the various apertures, biased surfaces and overall dimensions.**



**Figure 4. Instrument response for the X-, Y-, E-, and M-sweeps. For the X-sweep, the current plotted is the sum of both the bar and the collector current. For the other sweeps, only the collector current is analyzed. The vertical dashed line in each panel indicates where the embedded software has determined the current peak location.**

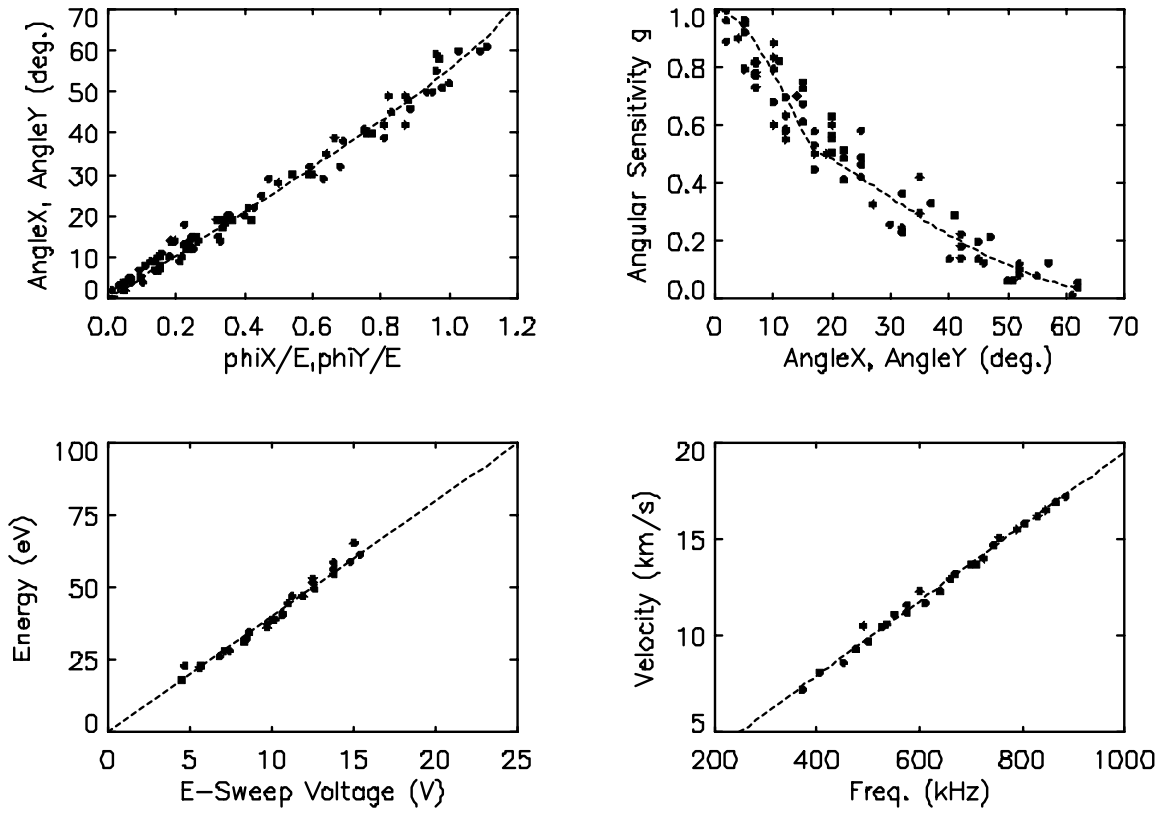


**Figure 5. Calibration data for angle, energy and velocity from the DPA instrument. Dashed lines are equations (1) – (4).**

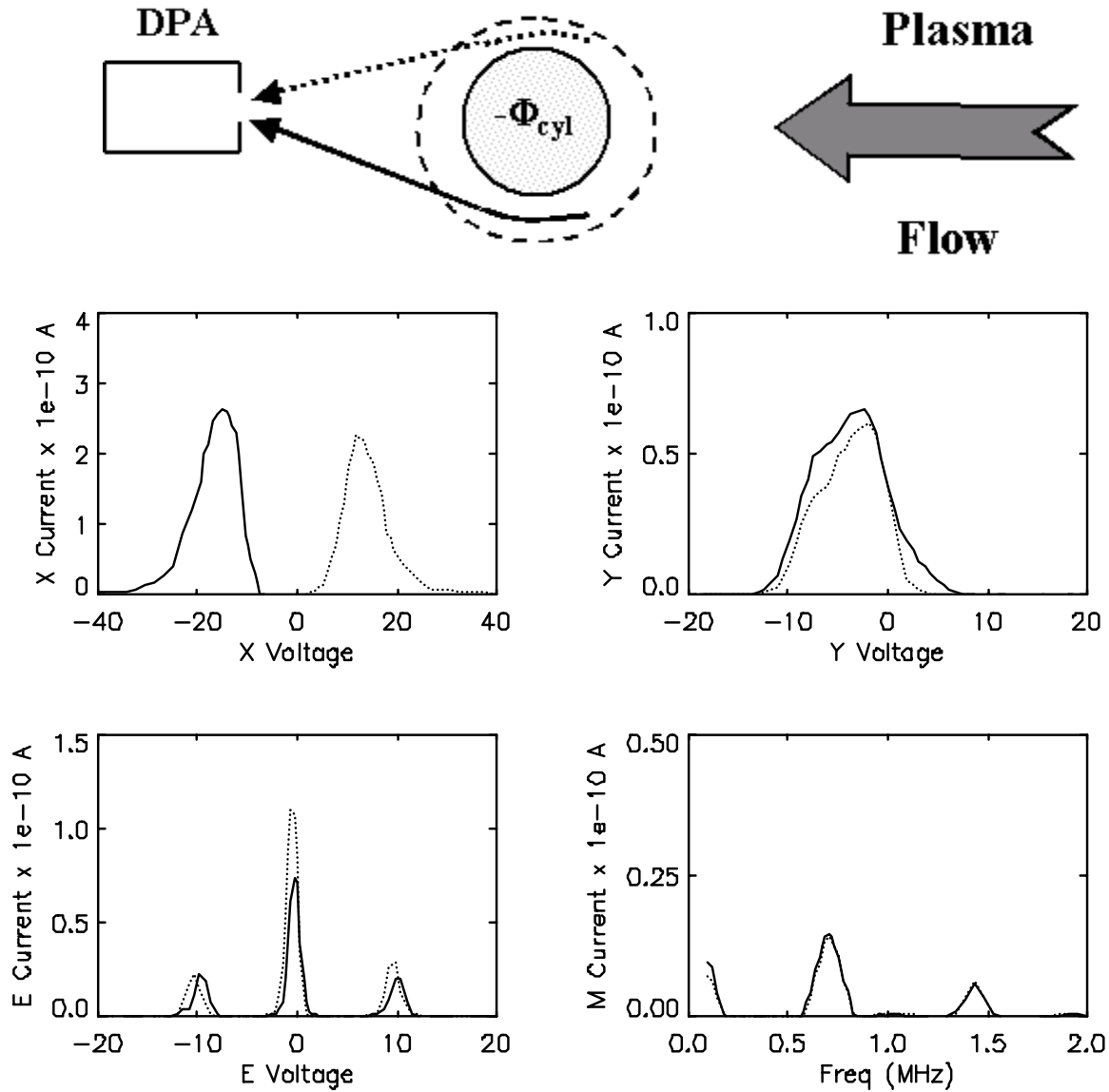


**Figure 6. Two stream data. Upper panel shows the experiment setup with plasma impinging on a negatively biased cylinder and deflection of the ion stream by the sheath around the cylinder. The plots in the lower part of the figure show the X-, Y-, E-, and M-sweep analysis of the two streams.**

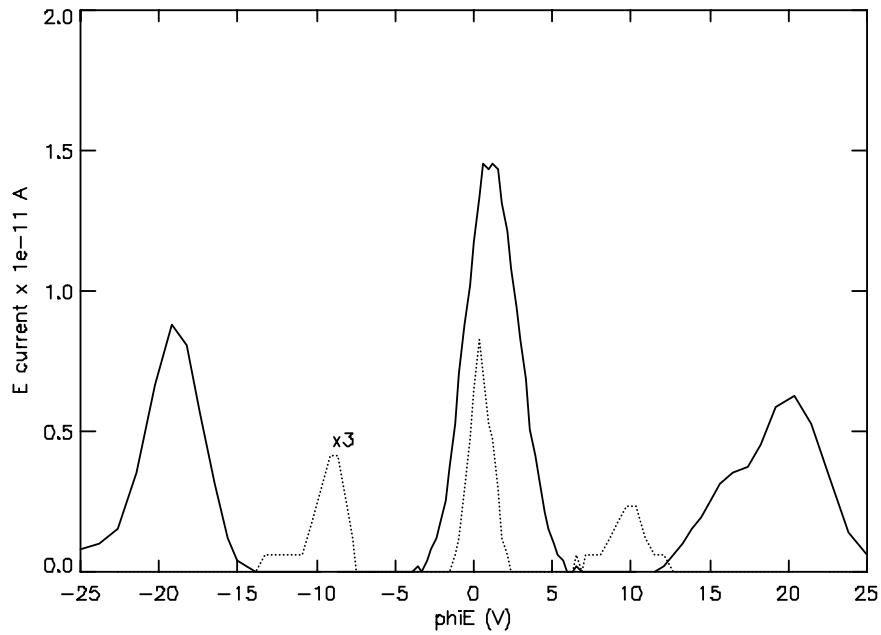
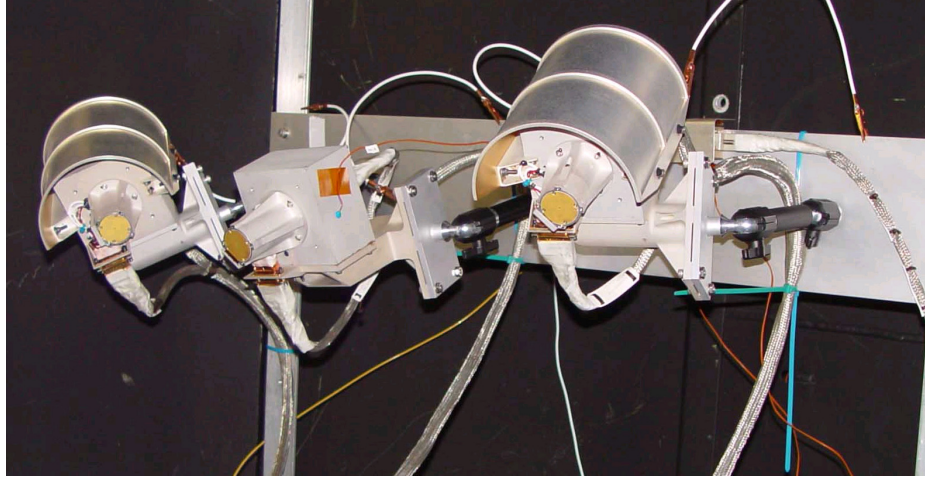


**Figure 7. Top panel: view of sensor set-up for system test. Bottom panel: response of DPA energy analysis for two system operating modes. Solid line is for shunt mode and dashed line for load resistor mode. In the shunt mode, a stream of  $\text{Xe}^+$  ions at density  $2 \times 10^5 \text{ cm}^{-3}$  and energy 77 eV were observed. In the load resistor mode, a stream of  $\text{Xe}^+$  ions at density  $1 \times 10^5 \text{ cm}^{-3}$  and energy 37 eV were observed.**

## References

1. Stone, N. H., Technique for measuring the differential ion flux vector, *Rev. Sci. Instrum.*, 48, 1458, 1977.
2. Stone, N. H., The plasma wake of mesosonic conducting bodies. Part 1. An experimental parametric study of ion focusing by the plasma sheath, *J. Plasma Phys.*, 25, 351, 1981.
3. Wright, K. H., Jr., N. H. Stone, and U. Samir, A study of plasma expansion phenomena in laboratory generated plasma wakes: Preliminary results, *J. Plasma Phys.*, 33, 71, 1985.
4. Wright, K. H., Jr., A study of single and binary ion plasma expansion into laboratory generated plasma wakes, NASA Contractor Report 4125, February, 1988.
5. Stone, N. H., B. J. Lewter, W. L. Chisholm, and K. H. Wright, Jr., Instrument for differential ion flux vector measurements on Spacelab 2, *Rev. Sci. Instrum.*, 56, 1897, 1985.
6. Stone, N. H., K. H. Wright, Jr., U. Samir, and K. S. Hwang, On the expansion of ionospheric plasma into the near wake of the space shuttle Orbiter, *Geophys. Res. Lett.*, 15, 1169, 1988.
7. Stone, N. H., K. H. Wright, Jr., J. D. Winningham, J. Biard, C. Gurgiolo, A technical description of the TSS-1 ROPE investigation, *Il Nuovo Cimento*, 17C, 85, 1994.
8. Wright, K. H., Jr., N. H. Stone, J. Sorensen, J. D. Winningham, C. Gurgiolo, Observations of reflected ions and plasma turbulence for satellite potentials greater than the ion ram energy, *Geophys. Res. Lett.*, 25, 417, 1998.
9. Stone, N. H., W. J. Raitt, and K. H. Wright, Jr., The TSS-1R electrodynamic tether experiment: Scientific and technological results, *Adv. Space Res.*, 24, 1037, 1999.
10. Khurana, K. K., M. G. Kivelson, T. P. Armstrong, and R. J. Walker, Voids in Jovian magnetosphere revisited: Evidence of spacecraft charging, *J. Geophys. Res.*, 92, 13399, 1987.
11. Pickett, J. S., G. B. Murphy, W. S. Kurth, C. K. Goertz, and S. D. Shawhan, Effects of chemical releases by the STS-3 Orbiter on the ionosphere, *J. Geophys. Res.*, 90, 3487, 1985.
12. Paterson, W. R. and L. A. Frank, Hot ion plasmas from the cloud of neutral gases surrounding the space shuttle, *J. Geophys. Res.*, 94, 3721, 1989.
13. Moore, T. E., Origins of magnetospheric plasma, U. S. Natl. Rep. Int. Union Geod. Geophys. 1987-1990, *Rev. Geophys.*, 29, 1039, 1991.
14. Stone, N. H., U. Samir, K. H. Wright, Jr., and K. S. Hwang, Comment on "Ram ion scattering by space shuttle  $V \times B$  induced differential charging" by I. Katz and V. A. Davis, *J. Geophys. Res.*, 93, 4143, 1988.

15. Katz, I. and V. A. Davis, Reply, *J. Geophys. Res.*, 93, 4149, 1988.
16. Johnson, L., R. D. Estes, E. Lorenzini, M. Martinez-Sanchez, and J. Sanmartin, Propulsive Small Expendable Deployer System Experiment, *J. Spacecr. Rockets*, 37, 173, 2000.